

# Phase Fluctuation Spectra: New Radio Science Information To Become Available in the DSN Tracking System Mark III-77

A. L. Berman  
TDA Engineering Office

*The DSN Tracking System Mark III-77 currently being implemented at the Deep Space Stations will automatically provide doppler noise (rms phase jitter) computed concurrently over three evenly spaced decades of data sample interval and associated time-scale:*

<i>Data sample interval, sec</i>	<i>Time-scale, sec</i>
0.1	1.8
1.0	18.0
10.0	180.0
100.0	1800.0

*It is here suggested that these data translate directly into "average" phase fluctuation spectra, and hence represent a new and convenient source of radio science information. Temporal phase fluctuation spectra derived from Viking and Helios doppler noise data yield a power law relationship with frequency as follows:*

$$P_{\phi}(f) \sim f^{-2.42}$$

*for the following approximate range of frequencies:*

$$3.3 \times 10^{-2} \text{ Hz} > f > 5.6 \times 10^{-4} \text{ Hz}$$

## I. Introduction

In early 1978, the DSN Tracking System Mark III-77 will initiate the continuous and automatic computation of doppler noise concurrently at four sample rate intervals evenly spanning three orders of magnitude:

0.1 sec  
1.0  
10.0  
100.0

The process used to compute the noise will be the same for all of the sample rate intervals and is characterized by

- (1) The number of contiguous doppler (frequency) samples used in each computation is fixed (at 18).
- (2) The noise is computed for a least squares linear curve fit to the (18) data samples.

The above process is similar to the process by which doppler noise is currently computed in the Network Operations Control Center (NOCC), the only exception being that the current algorithm uses 15 samples, versus 18 samples in the new algorithm. It is significant that the number of samples used for each of the different sample interval noise calculations is fixed, as this results in the time-scale of the noise observations being proportional to the data sample interval. As there is considerable interest in doppler phase fluctuation spectra, particularly during solar conjunctions, it is here suggested that "average" temporal doppler phase fluctuation spectra may be routinely available in the DSN Tracking System Mark III-77 and require little additional processing. Extraction of the basic (noise) data by the user would be from the Archival Tracking Data File (ATDF) of the Tracking Data Management System.

## II. Average Doppler Phase Fluctuation Spectra Computed from Viking and Helios Doppler Noise

In Ref. 1, R. Woo used dual S- and X-band closed loop doppler data from the Mariner-Venus-Mercury (MVM) spacecraft at a Sun-Earth-Probe (SEP) angle of  $\sim 11.5$  deg to obtain typical differenced S-X phase fluctuation spectra. It is here desired to investigate whether doppler noise relationships derived by this author and J. A. Wackley (Refs. 2, 3, and 4) yield comparable spectra information.

In Ref. 2, doppler noise was found to be functionally dependent upon sample interval (15 samples, least squares linear curve fit) as:

$$\text{Noise} \propto \left(\frac{60}{\tau}\right)^{0.285}; \text{ Helios}$$

$$\text{Noise} \propto \left(\frac{60}{\tau}\right)^{0.294}; \text{ Viking}$$

where  $\tau$  = data sample interval in seconds.

In the following analysis, a combined Helios and Viking noise variation with data sample interval will be utilized, as follows:

$$\text{Noise} \propto \left(\frac{60}{\tau}\right)^{0.29}$$

From Refs. 3 and 4 one has the following noise average values for  $\tau = 60$  seconds and at an SEP of  $11.5$  deg:

$$\text{Noise} = 0.023 \text{ Hz}; \text{ Helios}$$

$$\text{Noise} = 0.024 \text{ Hz}; \text{ Viking}$$

Likewise combining the above, one constructs a composite Helios and Viking noise relationship with data sample interval at an SEP of  $11.5$  deg of

$$\text{Noise}(\tau) = 0.0235 \left(\frac{60}{\tau}\right)^{0.29} \text{ Hz}$$

Obtaining the relationship between doppler noise and "rms phase fluctuation" presents some difficulty; previously (Ref. 5), it was assumed that:

$$\text{rms phase}(\tau) = \tau \text{ noise}(\tau)$$

To check this assumption, a phase fluctuation of the form:

$$\text{phase}(t) = \sin 2\pi (t/T + K)$$

$$T = \text{phase fluctuation period, Hz}^{-1}$$

$$K = \text{arbitrary phase, cycles}$$

was passed through a simulated model of the DSN Noise algorithm (but without the linear curve fit). The results are seen in Fig. 1, and indicate

$$\frac{1}{4} \leq \frac{\tau \text{ noise}(\tau)}{\text{rms phase}(\tau)} \leq \frac{9}{4}$$

for the range

$$\tau/2 \leq T \leq 30\tau$$

It will be assumed here that:

$$\frac{\tau \text{ noise } (\tau)}{\text{rms phase } (\tau)} \cong \frac{3}{5}$$

or

$$\text{rms phase } (\tau) \cong \frac{5}{3} \tau \text{ noise } (\tau)$$

for fluctuations in the region:

$$\tau/2 \leq T \leq 30\tau$$

Introducing a factor of  $\sqrt{2}$  to obtain a one-way spectrum from two-way doppler noise,

$$\begin{aligned} \text{rms phase } (\tau) &\cong \frac{1}{\sqrt{2}} \frac{5}{3} \tau \left[ 0.0235 \left( \frac{60}{\tau} \right)^{0.29} \right] \text{ Hz sec} \\ &= \frac{100}{\sqrt{2}} \left[ 0.0235 \left( \frac{60}{\tau} \right)^{0.29} \left( \frac{\tau}{60} \right) \right] \text{ cycles} \\ &= \frac{2.35}{\sqrt{2}} \left( \frac{\tau}{60} \right)^{0.71} \text{ cycles} \\ &= \sqrt{2} 2.35 \left( \frac{\tau}{60} \right)^{0.71} \text{ rad} \end{aligned}$$

and hence

$$\begin{aligned} \text{mean square phase} &= 2\pi^2 5.52 \left( \frac{\tau}{60} \right)^{1.42} \text{ rad}^2 \\ &= 109 \left( \frac{\tau}{60} \right)^{1.42} \text{ rad}^2 \end{aligned}$$

Now define the following:

$f$  = phase fluctuation frequency, Hz

$T$  = phase fluctuation period,  $\text{Hz}^{-1}$

$$T = f^{-1}$$

The least squares linear curve fit to the 15 data samples (substantially) "fits out" fluctuations with periods greater than  $T$  where:

$$T \cong 2 \times 15\tau = 30\tau$$

The mean square phase fluctuations in  $\text{rad}^2$  can then be considered:

$$\int_{(30\tau)^{-1}}^{(\tau/2)^{-1}} P_{\phi}(\nu) d\nu \approx \int_f^{\infty} P_{\phi}(\nu) d\nu$$

where

$$f = (30\tau)^{-1}$$

$P_{\phi}(f) \equiv$  temporal phase fluctuation spectra derived from doppler noise,  $\text{rad}^2 \text{ Hz}^{-1}$

so that

$$\begin{aligned} \int_f^{\infty} P_{\phi}(\nu) d\nu &\approx 109 \left( \frac{30\tau}{1800} \right)^{1.42} \text{ rad}^2 \\ &= 109(1800)^{-1.42} f^{-1.42} \text{ rad}^2 \\ &= 2.6 \times 10^{-3} f^{-1.42} \text{ rad}^2 \end{aligned}$$

Differentiating both sides with respect to  $f$ :

$$\begin{aligned} \frac{d}{df} \int_f^{\infty} P_{\phi}(\nu) d\nu &= -P_{\phi}(f) \text{ rad}^2 \text{ Hz}^{-1} \\ \frac{d}{df} 2.6 \times 10^{-3} f^{-1.42} &= -(1.42) 2.6 \times 10^{-3} f^{-2.42} \text{ rad}^2 \text{ Hz}^{-1} \\ &= -3.7 \times 10^{-3} f^{-2.42} \text{ rad}^2 \text{ Hz}^{-1} \end{aligned}$$

or

$$P_{\phi}(f) = 3.7 \times 10^{-3} f^{-2.42} \text{ rad}^2 \text{ Hz}^{-1}$$

For data sample intervals between 1 sec and 60 sec (from Ref. 2), the corresponding applicable frequency range is:

$$3.3 \times 10^{-2} \text{ Hz} > f > 5.6 \times 10^{-4} \text{ Hz}$$

Values of this average phase fluctuation spectrum for various frequencies are presented below:

$f, \text{ Hz}$	$P_{\phi}(f), \text{ rad}^2 \text{ Hz}^{-1}$
$10^1$	$1.4 \times 10^{-5}$
$10^0$	$3.7 \times 10^{-3}$
$10^{-1}$	$9.8 \times 10^{-1}$
$10^{-2}$	$2.6 \times 10^2$
$10^{-3}$	$6.7 \times 10^4$
$10^{-4}$	$1.8 \times 10^7$
$10^{-5}$	$4.7 \times 10^9$

Figures 2 and 3 are taken from Ref. 1 and are differenced S-X phase fluctuation spectra for the MVM spacecraft at an SEP of approximately 11.5 deg; overplotted on Figs. 2 and 3 is the doppler noise derived phase fluctuation spectrum at a similar SEP:

$$P_{\phi}(f) = 3.7 \times 10^{-3} f^{-2.42} \text{ rad}^2 \text{ Hz}^{-1}$$

The agreement between the two is seen to be quite reasonable; Woo (Ref. 1) indicates finding the relationship between the S-X differenced phase spectra ( $W_{\phi d}(f)$ ) and  $f$  to be:

$$W_{\phi d}(f) \sim f^{-2.5} \text{ to } f^{-2.6}$$

which is compared to the doppler noise derived phase fluctuation spectra

$$P_{\phi}(f) \sim f^{-2.42}$$

Table 1 presents a comparison of the frequency dependence of other determined or measured temporal solar plasma spectra (as computed from the equivalent power law three-dimensional spatial power spectra).

### III. Doppler Noise Derived Average Phase Fluctuation Spectra as a Function of SEP

The Viking data utilized in Ref. 2 spanned a range of SEP angle as follows:

$$6.4^\circ \geq \text{SEP} \geq 0.9^\circ$$

Figure 4 shows the exponent solutions from Table 2, Ref. 2, translated into average spectra as in Section II and plotted as a function of SEP. No significant correlation of spectral frequency dependence with SEP is seen. In Ref. 6, H. Chang hypothesizes that at low SEPs (hence strong scintillation) the temporal solar plasma spectra change from power law to exponential; the data in Fig. 4 do not appear to support this contention. It is here considered that doppler noise data may be quite useful in further study of phase fluctuation spectra (frequency dependence) as a function of SEP.

Combining the results of Section II with the ISEDC doppler noise model from Ref. 2, one can construct an average phase fluctuation spectrum as a function of the relevant geometry:

$$\begin{aligned} P_{\phi}(f, \alpha, \beta) &= \left[ \frac{\text{ISEDC Hz}}{0.0235 \text{ Hz}} \right]^2 3.7 \times 10^{-3} f^{-2.42} \text{ rad}^2 \text{ Hz}^{-1} \\ &= 6.7 f^{-2.42} \left( A_0 \left[ \frac{\beta}{(\sin \alpha)^{1.3}} \right] F(\alpha, \beta) \right. \\ &\quad \left. + A_1 \left[ \frac{1}{(\sin \alpha)^5} \right] \right)^2 \text{ rad}^2 \text{ Hz}^{-1} \end{aligned}$$

where

$$A_0 = 1.182 \times 10^{-3}$$

$$A_1 = 4.75 \times 10^{-10}$$

$\alpha$  = Sun-Earth-Probe angle, rad

$\beta$  = Earth-Sun-Probe angle, rad

$$\begin{aligned} F(\alpha, \beta) &= 1 - 0.05 \left[ \frac{(\beta - \pi/2 + \alpha)^3 - (\alpha - \pi/2)^3}{\beta} \right] \\ &\quad - 0.00275 \left[ \frac{(\beta - \pi/2 + \alpha)^5 - (\alpha - \pi/2)^5}{\beta} \right] \end{aligned}$$

## IV. Summary

It is here suggested that average phase fluctuation spectra can be easily obtained from doppler noise computed concurrently over different time scales. Using such data from the Viking and Helios solar conjunctions, an average phase fluctuation spectrum at 11.5 deg SEP is calculated to be

$$P_{\phi}(f) = 3.7 \times 10^{-3} f^{-2.42} \text{ rad}^2 \text{ Hz}^{-1}$$

and can be extrapolated to the full range of SEP via the ISEDC doppler noise model. Concurrent doppler noise computations at four evenly decade separated data sample intervals

$$0.1 \text{ sec} \leq \tau \leq 100.0 \text{ sec}$$

combined with a least squares linear curve fit are expected to provide average phase fluctuation spectra data for the frequency range:

$$2.8 \times 10^{-1} \text{ Hz} > f > 2.8 \times 10^{-4} \text{ Hz}$$

It is expected that these data may be quite useful in studying the frequency dependence of phase fluctuation spectra as a function of SEP, particularly at low SEPs ( $\leq 5^\circ$ ) for which there currently exist few published results.

Concurrent computation of doppler noise estimations is being implemented as a standard and automatic capability of the DSN Tracking System Mark III-77 and will become routinely and conveniently available to users in early 1978.

## Acknowledgment

I am indebted to L. Y. Lim, who graciously simulated the DSN doppler noise model and plotted the output via the very efficient MBASIC\* language.

---

\*A trademark of the California Institute of Technology.

## References

1. Woo, R., Yang, F., Yip, K. W., and Kendall, W. B., "Measurements of Large Scale Density Fluctuations in the Solar Wind Using Dual Frequency Phase Scintillations", *Ap. J.*, 210, Jan. 1977.
2. Berman, A. L., "A Comprehensive Two-Way Doppler Noise Model for Near-Real-Time Validation of Doppler Data," in *The Deep Space Network Progress Report 42-37*, Jet Propulsion Laboratory, Pasadena, Calif., Feb. 15, 1977.
3. Berman, A. L., Wackley, J. A., and Rockwell, S. T., "The 1976 Helios and Pioneer Solar Conjunctions – Continuing Corroboration of the Link Between Doppler Noise and Integrated Signal Path Electron Density," in *The Deep Space Network Progress Report 42-36*, Jet Propulsion Laboratory, Pasadena, Calif., Dec. 15, 1976.
4. Berman, A. L., and Wackley, J. A., "Viking S-Band Doppler RMS Phase Fluctuations Used to Calibrate the Mean 1976 Equatorial Corona," in *The Deep Space Network Progress Report 42-38*, Jet Propulsion Laboratory, Pasadena, Calif., Apr. 15, 1977.
5. Berman, A. L., "Proportionality Between Doppler Noise and Integrated Signal Path Electron Density Validated by Differenced S/X Range," in *The Deep Space Network Progress Report 42-38*, Jet Propulsion Laboratory, Pasadena, Calif., Apr. 15, 1977.
6. Chang, H., "Analysis of Dual-Frequency Observations of Interplanetary Scintillations Taken by The Pioneer 9 Spacecraft," Doctoral dissertation, Department of Electrical Engineering, Stanford University, May 1976.

**Table 1. Typical values of the logarithmic slope of temporal solar plasma spectra with frequency <sup>a</sup>**

Source	Reference	$\text{Log } P_{\phi}(\nu)/\text{Log } \nu$	Frequency range ( $\nu$ ), Hz	Distance (closest approach or in situ), AU	Measurement
Berman		-2.42	$3.3 \times 10^{-2} > \nu > 5.6 \times 10^{-4}$	0.016-0.111	S-band doppler noise
Woo et al.	1	-2.5/-2.6	$5 \times 10^{-1} > \nu > 1 \times 10^{-4}$	0.2	Differenced S- and X-band phase
Chang	6	-2.5	$1 \times 10^1 > \nu > 1 \times 10^0$	0.1-1	Dual-frequency interplanetary scintillation (IPS)
Unti et al.	6	-2.55	$1.3 \times 10^1 > \nu > 5 \times 10^{-3}$	~1	In situ proton density
Intriligator and Wolfe	6	-2.3	$1 \times 10^{-3} > \nu > 1 \times 10^{-4}$	~1	In situ proton density
Coleman	6	-2.2	$1 \times 10^{-2} > \nu > 1 \times 10^{-5}$	0.9-1	In situ magnetic field and plasma velocity spectra

<sup>a</sup> Assumes the temporal (columnar) spectrum is proportional to  $\nu^{-(x-1)}$  if the three-dimensional spatial power spectrum is power law with exponent  $-x$ .

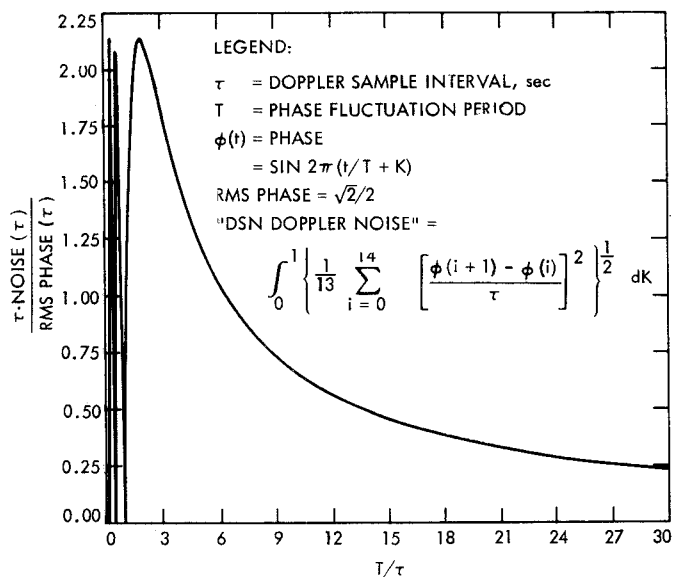


Fig. 1. Ratio of DSN doppler noise to rms phase fluctuation as a function of phase fluctuation frequency

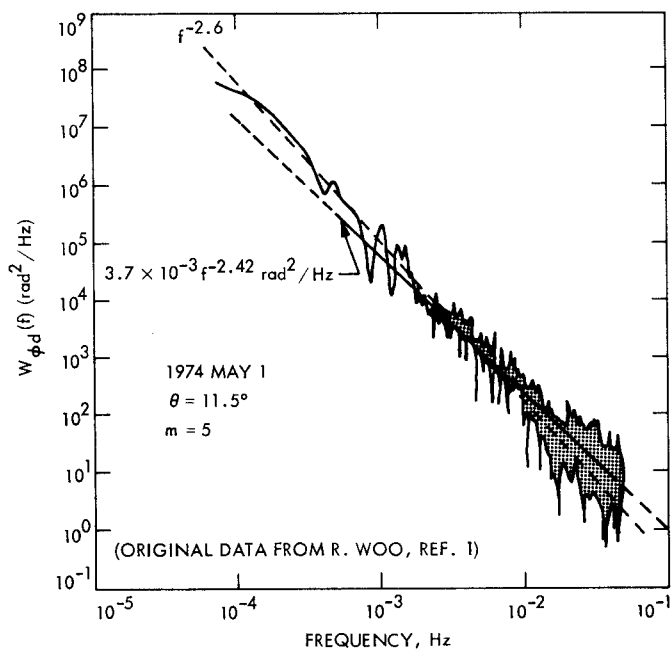


Fig. 3. Comparison of MVM differenced phase spectra to Viking-Helios doppler noise phase fluctuation spectra

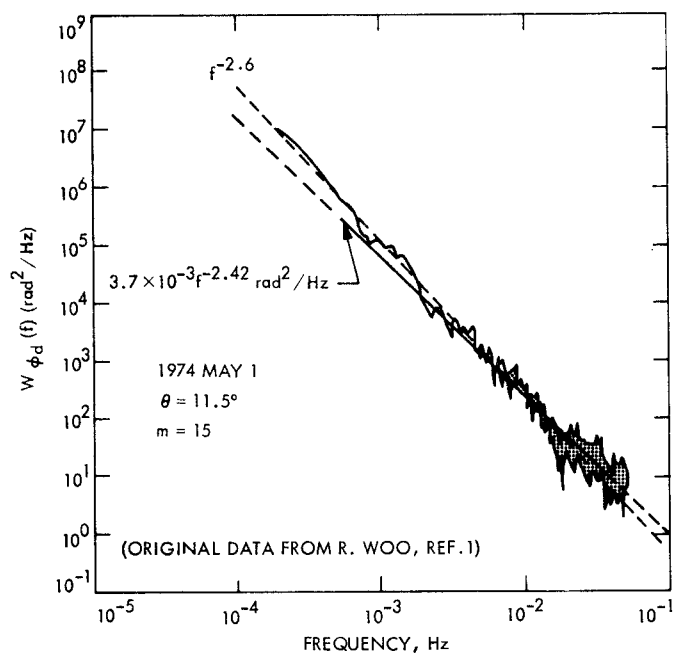


Fig. 2. Comparison of MVM differenced phase spectra to Viking-Helios doppler noise phase fluctuation spectra

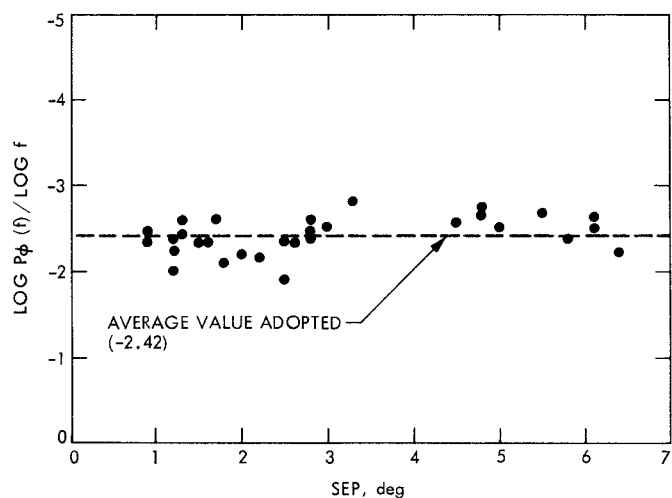


Fig. 4. Logarithmic slope of phase fluctuation spectra vs frequency as determined from Viking doppler noise